

# Same but Different: distance correlations between topological summaries

Katharine Turner and Gard Spreemann

December 15, 2024

## Abstract

Persistent homology allows us to create topological summaries of complex data. In order to analyse these statistically we need to choose a topological summary and a metric space where these topological summaries exist. While different representations of the persistent homology may contain the same information (as they come from the same persistence module) they can lead to different statistical conclusions because the metric spaces they lie in are different. The best choice for analysis will be application specific. In this paper we will discuss distance correlation which is a non-parametric tool for comparing data sets that can lie in completely different metric spaces. In particular we can calculate the distance correlation between different choices of topological summary (e.g. bottleneck distance persistence diagrams vs  $L^2$  function distances between persistence landscapes). For a variety of random models we compare some different topological summaries via the distance correlation between the samples. We will give examples of performing distance correlation between topological summaries to another measurement of interest - such as a paired random variable or a parameter in the random model used to generate the persistent homology. This article is meant to be expository in style, so we will include the definitions of standard statistical quantities to make the paper accessible to non-statisticians.

## 1 Introduction

The development and application of statistical theory and methods within Topological Data Analysis (TDA) is still in its infancy. The main reason is that distributions of topological summaries will not be as easy to study as distributions of real numbers, or even of vectors. There are complications that arise from the geometry and topology of the spaces that these summaries lie in, and perhaps more importantly there is a complete lack of nice parameterised families which could expect the distributions of topological summaries to follow. Even when the distribution of filtrations of topological spaces is parametric, the process of computing topological summaries is generally very non-linear so the resulting topological summaries will probably not be in the form of a tractable exponential family. Effectively none of the methods from a first year statistics course can be directly applied - at least not without significant caveats. We instead turn to the world of non-parametric statistics. Here the methods are usually distribution free and sometimes can be applied to random elements lying in quite general metric spaces.

A quintessential example of the challenges that TDA faces in improving its statistical rigour is correlation. The Pearson correlation coefficient is the correlation, the “r-value”, taught in every introductory course on statistics. However, it is only defined for real valued functions and is designed to be used for normal distributions. It measures the strength of the linear relationship between normally distributed variables. The parametric families are the normal distributions with parameters the mean and covariance matrices and the correlation coefficient is a straightforward formula from the covariance matrix. Pearson correlation is very useful and appropriate if the distributions are normal real valued random variables. But that is a very big “if”; and one that will rarely hold for topological summaries.

Thankfully for TDA, correlation as a concept is not defined by the formula of the Pearson correlation coefficient but instead can be considered as some quantity measuring the extent of interdependence of variables. This

research is the result of a treasure hunt within the field of non-parametric statistics for an appropriate notion of correlation applicable to topological summaries. Our finding was distance correlation (see Definition 2.3). Effectively distance correlation looks at the correlations between pairwise distances (appropriately recentred) instead of the raw values. This makes it very generally applicable - it can be applied to distributions over any pair of metric spaces!

Distance correlation also encapsulates the non-parametric approach of being distribution free. It can detect relationships between variables that are not linear, and not even monotonic. If the variables are independent then the distance correlation is zero. In the other direction, if the metrics spaces are of strong negative type (see Definition 2.5) then distance correlation of 0 implies the variables are independent. This is true for any joint distribution. In contrast, we can only conclude from Pearson correlation coefficient being zero that the variables are independent when we can assume that the joint distribution is bivariate normal.

There are two take-home messages. The first is that distance correlation is a useful tool in the statistical analysis of topological summaries. The current exposition serves as an introduction to the potential of distance correlation for statistical analysis in TDA. In the future directions we outline some further opportunities that distance correlation can offer. The second message is the simple observation that the choice of topological summary statistic matters. A responsible topological data analyst should consider which is the most appropriate topological summary. A better choice of summary is one where the pairwise distances better reflect the differences in the raw data that are of interest. This will be domain and application specific. There may be other considerations for topological summary choice in terms of statistical methods available, computational complexity and inference power, but this is beyond the scope of the present discussion.

## 2 Background theory

### 2.1 Topological summary statistics

TDA is usually concerned with analysing complex data. This data may have complicated geometric or topological structure and we can create a family of topological spaces as a way of representing this structure. We call a family of spaces  $\{K_a\}_{a \in A \subset \mathbb{R}}$  a *filtration* if  $K_a \subset K_b$  whenever  $a \leq b$ . The inclusion of  $K_a \subset K_b$  induces a homomorphism between the homology groups  $H_k(K_a)$  and  $H_k(K_b)$ . The persistent homology group is the image of  $H_k(K_a)$  in  $H_k(K_b)$ , it encodes the  $k$ -cycles in  $K_a$  that are independent with respect to boundaries in  $K_b$ :

$$H_k(a, b) := Z_k(K_a) / (B_k(K_b) \cap Z_k(K_a)). \quad (2.1)$$

The two most common ways of representing persistent homology information are the barcode and the persistence diagram. The barcode is a collection of intervals  $[birth, death)$  each representing the birth, and death, values of a persistent homology class. This collection of intervals satisfy the condition that for every  $a \leq b$ , The number of intervals containing  $[a, b)$  is  $\dim(H_k(a, b))$ . The corresponding persistence diagram is the multi-set of points in the plane where each bar in the barcode is sent to the point with first coordinate its birth time and its second coordinate its death time.

A *summary statistic* is a object that is used to summarise a set of observations, in order to communicate the largest amount of information as simply as possible. Simple examples in the case of real valued distributions are the mean, variance, median and box plot. In TDA we can create summary statistics via persistent homology. We have a filtration of topological spaces built from our observations, and by applying persistent homology we can summarise this filtration in terms of the evolution of homology. Notably, here we are creating a summary from a single complex object, whether it be a point cloud, a graph, etc.

There are now a wide array of topological summaries that can be computed directly from a persistence diagram or barcode. Each of these is a different expression of the persistent homology in the form of a topological summary statistic. For the practitioner wanting to use perform statistical analysis using topological summaries, they need to choose which type of summary to represent their data and the metric on that space of summaries. For some of these different topological summaries there are parameters to choose which play the role of bandwidth, and some

depend on a choice of  $p$  (for us  $p \in \{1, 2, \infty\}$ ) which is the either exactly or analogously the index  $p$  in the  $L^p$  distance for function spaces.

In this paper we will consider a range of different topological summaries. These are

- Persistence diagrams, with Wasserstein distances for  $p = 1, 2$  and  $\infty$
- Persistence Landscapes, with  $L^p$  distances for  $p = 1, 2$  and  $\infty$
- Persistence scale space kernel, with two different bandwidths, with  $L^2$  distances
- Betti and Euler curves with  $L^p$  functional distances for  $p = 1, 2$
- Sliced Wasserstein kernel distance

Note that all of these topological summaries can be computed directly from the persistence diagram and that with the exception of the Betti and Euler curves they contain all the information of the original persistence diagram. In this sense they are the “same”. It is merely the metric space structure that is different.

It is worth noting that the above list is by no means an exhaustive list of topological summaries. Other examples of topological summaries include the persistent homology rank function [21], the accumulation persistence function [4], the Persistence Weighted Gaussian Kernel [12], the persistence Fisher kernel [13], using tangent vectors from the mean of the square-root framework with principal geodesic analysis [2], using points in the persistence diagrams as roots of a complex polynomial for concatenated-coefficient vector representations [9], or using distance matrices of points in persistence diagrams for sorted-entry vector representations [8]. Notably most of these are all functional summaries with an  $L^2$  metric or lie in a reproducing kernel Hilbert space. Analogous arguments to those for the persistence scale shape space discussed later could be used to show that many of them lie in metric spaces of strong negative type as a corollary of being separable Hilbert spaces.

## 2.2 Pearson Correlation vs Distance Correlation

A *random element* is a map from a probability space  $\Omega$  to a set  $\mathcal{X}$ . Its *distribution* is the pushforward measure onto  $\mathcal{X}$ . Given two random elements  $X : \Omega \rightarrow \mathcal{X}$  and  $Y : \Omega \rightarrow \mathcal{Y}$  can consider the paired samples  $(X, Y) : \Omega \rightarrow \mathcal{X} \times \mathcal{Y}$ . This has a *joint distribution* on  $\mathcal{X} \times \mathcal{Y}$ . The *marginal distributions* for this joint distribution are the pushforwards via to projection maps onto each of the coordinates. An important notion in statistics is when two variables are *independent*. This occurs precisely when the joint distribution is the product of the marginal distributions.

The most common measure of correlation is the Pearson correlation coefficient. This is defined as the covariance of the two variables divided by the product of their standard deviations. For paired random variables  $X, Y$ , the Pearson correlation coefficient is defined by the equation

$$\rho_{X,Y} = \frac{\mathbb{E}[(X - \bar{X})(Y - \bar{Y})]}{\sigma_X \sigma_Y}$$

where  $\bar{X}, \bar{Y}$  are the means of  $X$  and  $Y$ ,  $\sigma_X, \sigma_Y$  their standard deviations, and  $\mathbb{E}$  denotes expectation. Note that if  $X$  and  $Y$  are independent then  $\mathbb{E}[(X - \bar{X})(Y - \bar{Y})] = \mathbb{E}[(X - \bar{X})]\mathbb{E}[(Y - \bar{Y})] = 0$ . This implies that that non-zero correlation is evidence of a lack of independence, and hence the variables are somehow related (though possibly only indirectly).

Pearson correlation is designed to analyse bivariate Gaussian distributions. In this case a correlation of 0 implies that the variables are independent. Furthermore Pearson correlation determines the ellipticity of the distribution. We can calculate the Pearson correlation for more general distributions and here it detects linear relationships and nonlinear relationships can be lost. Some examples of the Pearson correlation coefficient are illustrated in Figure 1. Any test using the correlation coefficient (such as significance testing) depends on the bivariate Gaussian assumption.

In parametric statistics we make some assumption about the parameters (defining properties) of the population distribution(s) from which the data are drawn, while in non-parametric statistics we do not make such assumptions. Given the lack of parametric families of topological summaries statistics it makes sense to consider non-parametric methods. One option when studying real-valued random variables which are not normally distributed or the relationship between the variables is not linear there are to use the rankings of the samples. In particular the Spearman rank correlation method is commonly used. While these methods are distribution free, they are not suitable for topological summaries as the summaries do not lie in spaces with an order. We cannot rank the samples so we can't apply tests that use the ranks. It should also be mentioned that such ranking correlations are designed to detect monotone relationships, which although more general than the linearity of Pearson's correlation is still a significant restriction.

A new exciting non parametric alternative is to work with the pairwise distances. Given paired samples  $(X, Y) = \{(x_i, y_i) \mid i = 1, \dots, n\}$  where the  $x_i$  and  $y_i$  lie in metric spaces  $\mathcal{X}$  and  $\mathcal{Y}$  we can ask what the joint variability is of the pairwise distances (that is how related is  $d_{\mathcal{Y}}(y_i, y_j)$  to  $d_{\mathcal{X}}(x_i, x_j)$ ). The statistical tools of distance covariance and distance correlation are apt for this purpose. This notion was introduced in [23] in the case of samples lying in Euclidean space, where they showed that it can test independence with distance correlation of zero if and only if the variables were independent. This made no assumptions on the distributions and can detect relationships that are highly nonlinear. In contrast, we can only conclude from Pearson correlation coefficient begin zero that the variables are independent when we can assume that the joint distribution is bivariate normal. This difference between Pearson correlation and distance correlation is illustrated with real valued random variables in Figure 1.

Distance correlation can be applied to distributions of samples lying in more general metric spaces. It can detect relationships between variables that are not linear, and not even monotonic. This can be seen in Figure 2.2. There are strong theoretical results about independence.

**Theorem 2.1.** [15] *If the variables are independent then the distance correlation is zero. In the other direction, if the metrics spaces are separable and of strong negative type then distance correlation of 0 implies the variables are independent. This is true for any joint distribution.*

**Definition 2.2.** Let  $X$  be a random element with values in a connected metric space  $(\mathcal{X}, d_{\mathcal{X}})$  with distribution  $\mu$ . For  $x \in \mathcal{X}$  we call  $\mathbb{E}[d_{\mathcal{X}}(x, X)]$  the *expected distance* of  $X$  to  $x$ , and denote it by  $a_{\mu}(x)$ . We say that  $X$  has *finite first moment* if for any  $x \in \mathcal{X}$  the expected distance to  $x$  is finite. In this case we can then set  $D(\mu) := \mathbb{E}[a_{\mu}(X)]$ . For  $X$  with finite first moment we can define its *doubly centred distance function* as

$$d_{\mu}(x, x') := d_{\mathcal{X}}(x, x') - a_{\mu}(x) - a_{\mu}(x') + D(\mu).$$

It is worth observing that  $d_{\mu}$  is not a distance function. Lyons showed in [15] that  $a_{\mu}(x) > D(\mu)/2$  for all  $x$  as long as the support of  $\mu$  contains at least two points. This implies  $d_{\mu}(x, x) < 0$  for all  $x$ .

**Definition 2.3.** Let  $\mathcal{X}$  and  $\mathcal{Y}$  be metric spaces. Let  $\theta = (X, Y)$  be a probability distribution over the product space  $\mathcal{X} \times \mathcal{Y}$  with marginals  $\mu$  and  $\nu$  such that  $X$  and  $Y$  both have finite first moment. We define the *distance covariance* of  $\theta$  as

$$\text{dcov}(\theta) = \int d_{\mu}(x, x') d_{\nu}(y, y') d\theta^2((x, y), (x', y'))$$

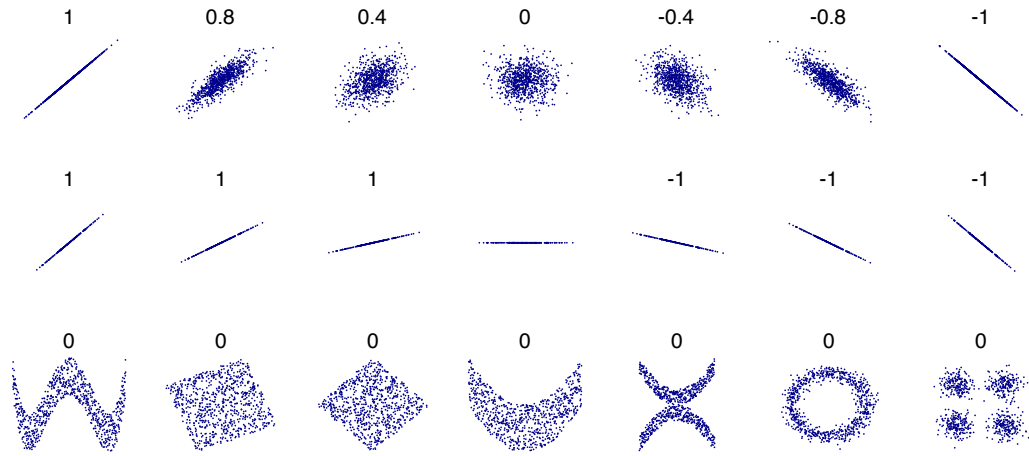
The *distance variance* is a special case where have two identical copies as the joint distributions  $\theta^X = (X, X)$ . Here we have

$$\text{dvar}(\theta^X) = \int d_{\mu}(x, x')^2 d\theta^2((x, x'))$$

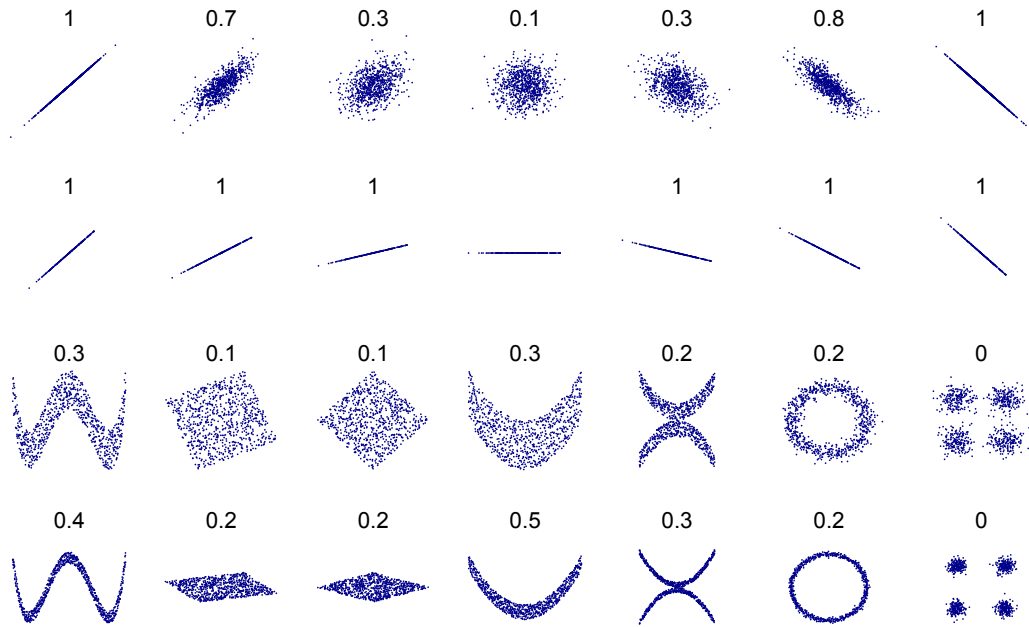
which is always non-negative, and zero only in the case of a distribution with support a single point (see [15]).

The *distance correlation* of  $\theta = (X, Y)$  is defined as

$$\text{dcor}(X, Y) = \frac{\text{dcov}(X, Y)}{\sqrt{\text{dvar}(\theta^X) \text{dvar}(\theta^Y)}}.$$



(a) Pearson Correlation



(b) Distance Correlation

Figure 1: These examples demonstrate how distance correlation is much more useful when the joint distribution is not a multivariate Gaussian. Image source: wikipedia [27, 28]

*Remark.* There are some variations of notation with regard to whether to include a square root in the definition of distance covariance and correlation. In the introduction of distance correlation in [23], the authors restricted to Euclidean spaces. Euclidean spaces are metric spaces of negative type, and such spaces have the property that the distance correlation is always non-negative. They could thus define the distance covariance as

$\sqrt{\int d_\mu(x, x')d_\nu(y, y')d\theta^2((x, y), (x', y'))}$ . We will follow the notation of [15] and use  $\text{dCov}$  to denote the square root of  $\text{dcov}$ ;  $\text{dCov}(X, Y) = \sqrt{\text{dcov}(X, Y)} = \sqrt{\int d_\mu(x, x')d_\nu(y, y')d\theta^2((x, y), (x', y'))}$ . We will also use  $\text{dVar}$  as the square root of the distance variation and  $\text{dCor}$  to denote the square root of the distance correlation, which is  $\text{dCor}(X, Y) = \text{dCov}(X, Y) / \sqrt{\text{dVar}(X)\text{dVar}(Y)} = \sqrt{\text{dcor}(X, Y)}$ . In the simulations and calculations involving topological summaries, it turns out that all the values of the distance correlation are non-negative, even for those involving spaces that are not of negative type.

**Definition 2.4.** Given a set of paired samples drawn from a joint distribution, we can compute a *sample distance covariance*. This is an estimator of the distance covariance of a joint distribution from which the paired samples was taken.

The estimation of the distance correlation of a joint distribution by sample distance covariances is reasonable. In other more technical words this means that if  $\theta_n$  is the sampled joint distribution from  $n$  iid sample of  $\theta$  then  $\text{dcov}(\theta_n) \rightarrow \text{dcov}(\theta)$  with probability 1. (See Proposition 2.6 in [15]). This justifies the approximation of the distance correlation via simulations. This is particularly important when dealing with distributions for which there is no closed expressions, which is usually the case when dealing with topological summaries

The following procedure computes the sample distance covariance between paired samples  $(X, Y) = \{(x_i, y_i) \mid i = 1, \dots, n\}$  which we denote  $\text{dcov}_n(X, Y)$ . It is the straightforward implementation of the definition.

1. Compute the pairwise distance matrices  $(a_{ij})$   $(b_{ij})$  with  $a_{ij} = d_X(x_i, x_j)$  and  $b_{ij} = d_Y(y_i, y_j)$ .
2. Compute the means of each row and column in  $A$  and  $B$  as well as the total means of the matrices. Let  $\bar{a}^i$  and  $\bar{b}^i$  denote the row means and  $\bar{a}_j$  and  $\bar{b}_j$  the column means. Let  $\bar{a}$  and  $\bar{b}$  denote the matrix means.
3. Compute doubly centered matrices  $(A_{kl})$  and  $(B_{kl})$  with  $A_{kl} = a_{kl} - \bar{a}^k - \bar{a}_l + \bar{a}$  and  $B_{kl} = b_{kl} - \bar{b}^k - \bar{b}_l + \bar{b}$
4. The sample distance covariance is

$$\text{dcov}_n = \frac{1}{n^2} \sum_{k,l=1}^n A_{kl}B_{kl}$$

Note that the matrices  $A$  and  $B$  have the property that all rows and columns sum to zero. .

## 2.3 Metric spaces of strong negative type

As straightforward application of the definition shows that the distance correlation of a product measure is always zero. To see this observe that when  $\theta$  is a product of  $\theta_X$  and  $\theta_Y$  then

$$\text{dcov}(\theta) = \int d_\mu(x, x')d_\nu(y, y')d\theta^2((x, y), (x', y')) = \int d_\mu(x, x')d\theta_X^2(x, x') \int d_\nu(y, y')d\theta_Y^2(y, y')$$

and by construction of  $d_\mu$  and  $d_\nu$ , we have  $\int d_\mu(x, x')d\theta_X^2(x, x') = 0 = \int d_\nu(y, y')d\theta_Y^2(y, y')$ . The converse of this statement holds under conditions on the metric spaces the distributions are over (and not the distributions themselves).

**Definition 2.5.** A metric space  $(X, d)$  has *negative type* if for all  $x_1, \dots, x_n \in X$  and  $\alpha_1, \alpha_2, \dots, \alpha_n$  such that  $\sum_i \alpha_i = 0$  we have  $\sum_{i,j=1}^n \alpha_i \alpha_j d(x_i, x_j) \leq 0$ .

Note that the definition of negative type coincides with that of conditionally negative semidefinite.

184 **Proposition 2.6.** [15] For spaces of negative type it is always true that distance covariance is non-negative.

185 We have further nice properties when the metric space is of strong negative type

**Definition 2.7.** A metric space has *strict negative type* is a space of negative type and if  $x_1, \dots, x_n \in X$  and  $\alpha_1, \alpha_2, \dots, \alpha_n$  such that  $\sum_i \alpha_i = 0$  and  $\sum_{i,j=1}^n \alpha_i \alpha_j d(x_i, x_j) = 0$  then the  $\alpha_i$  are all zero. By extending to distributions of infinite support we get the definition of strong negative type. A metric space  $(\mathcal{X}, d)$  has *strong negative type* if it has negative type and for all probability measures  $\mu_1, \mu_2$  we have

$$\int d(x, x') d(\mu_1 - \mu_2)^2(x, x') \leq 0$$

186 The notion of strong negative type was first defined in [29]. Lyons [15] used it to characterize the spaces where  
187 that we can test for independence of random variables. The challenge is then how to implement such a test given  
188 a sample distance correlation which will probably not be zero even when the variables are independent.

189 **Theorem 2.8.** [15] Suppose that  $\mathcal{X}$  and  $\mathcal{Y}$  have strong negative type and  $\theta$  is a probability measure on  $\mathcal{X} \times \mathcal{Y}$   
190 whose marginals have first finite moment. If  $\text{dcov}(\theta) = 0$  then  $\theta$  is a product measure.

191 This means that given paired random variable  $(X, Y)$  with joint distribution  $\theta$  then we can test for independence  
192 by computing  $\text{dcov}(\theta)$  and deciding they are independent if  $\text{dcov}(\theta) = 0$  and not independent if  $\text{dcov}(\theta) > 0$ .  
193 There are a range of spaces that are proven to be of strong negative type, including all separable Hilbert spaces.

194 **Theorem 2.9.** [15] Every separable Hilbert space is of strong negative type and if  $(X, d)$  has negative type, then  
195  $(X, d^r)$  has strong negative type when  $0 < r < 1$ .

196 A list of metric spaces of negative type appears as Theorem 3.6 of [16]; in particular, this includes all  $L^p$  spaces for  
197  $1 \leq p \leq 2$ . On the other hand,  $\mathbb{R}^n$  with the  $l^p$ -metric is not of negative type whenever  $3 < n < \infty$  and  $2 < p < \infty$ .

198 The distance correlation still contains useful information even when the spaces are not of strong negative type. It  
199 is just more powerful as a test statistic when the spaces are of strong negative type. This is analogous to how the  
200 Pearson correlation coefficient still is evidence of a relationship between two variables even when the joint  
201 distribution is not Gaussian. Here the Pearson correlation coefficient is detecting linear relationships. It is an  
202 open question to characterise what relationships are detected via distance correlation in spaces that are not of  
203 strong negative type and what kinds of relationships are not detected.

204 Distance correlation lends itself to non-parametric methods. One possibility is to combine it with permutation  
205 tests to construct  $p$ -values for independence. Permutation tests construct a sampling distribution by resampling  
206 the observed data. We can permute the observed data without replacement to create a null distribution (in this  
207 case a distribution of distance correlation values under the assumption that the random variables are  
208 independent.) The use and exploration of permutation tests in relation to distance correlation is beyond the scope  
209 of this paper. We direct the interested reader to the future directions section for more details.

### 210 3 A veritable zoo of topological summaries and which are of strong 211 negative type

212 Persistent homology has become a very important tool in TDA. Certainly there are many choices that are made in  
213 any persistent homology analysis with much of the focus lying on the different options of the filtration function.  
214 In this paper we want to highlight another choice - the metric space of the topological summary we use. Examples  
215 include persistence diagrams with bottleneck distance, persistence landscapes or rank function with an  $L^p$   
216 distance, or one of the many kernel representations. The choice of which topological summary we use to represent  
217 this persistent homology, and the choice of metric in this space of topological summaries will affect any statistical  
218 analysis and whether the summary captures the information of relevance to the application.

For spaces of strong negative type, distance correlation is known to have the additional nice properties. As a rule, functional spaces with an  $L^2$  metric and those lying in a reproducing kernel Hilbert space are of strongly negative type. This implies that the Euler and Betti curves with an  $L^2$  metric are of strong negative type, and that the space of persistence scale shape kernels is of strong negative type. We characterise which of the spaces of persistence landscapes are of strong negative type and show that the space of persistence diagrams is never of strong negative type.

**Theorem** (Theorem 3.2). *The space of persistence diagrams is not of negative type under the bottleneck or any of the Wasserstein metrics.*

**Theorem** (Theorem 3.4). *We can prove the following statements about which metrics for the space of persistence landscapes is of negative type and of strong negative type.*

- (a) *The space of persistence landscapes with the  $L^2$  norm of strong negative type.*
- (b) *The space of persistence landscapes with the  $L^p$  norm of negative type when  $1 \leq p \leq 2$*
- (c) *The space of persistence landscapes with the  $L^1$  norm is not of strong negative type, even when restricting to persistence landscapes that arise from persistence diagrams.*
- (d) *The space of persistence landscapes with the  $L^\infty$  norm is not of negative type, even when restricting to persistence landscapes that arise from persistence diagrams.*

It is an open question as to whether the Sliced Wasserstein metric is of strong negative type; if it is separable then it will be.

### 3.1 Betti and Euler curves

One of the first topological summaries considered for parameterised families of topological spaces  $(\{K_a\})$  are the Betti and the Euler curves, which we denote by  $\beta_k$  and  $\chi$ . These are integer valued functions with  $\beta_k(a) = \dim H_k(K_a)$  and  $\chi(a) = \chi(K_a)$ . These can be computed from a barcode as  $\beta_k(a)$  is the number of bars that contain the point  $a$ . We can compute  $\chi(a)$  as the alternating sum of the Betti numbers  $\chi(a) = \sum_{k=0}^{\infty} (-1)^k \beta_k(a)$ .

Note that the Betti curves do not contain the “same” information as the persistence diagrams but instead contain strictly less information.

We can consider functional distances between these curves. In this paper we consider both  $L^1$  and  $L^2$  distances. Since  $L^2(\mathbb{R})$  is a separable Hilbert space it is of strong negative type. In comparison  $L^1(\mathbb{R})$  is of negative type but not of strict negative type (see [15]). For an explicit counterexample the reader can modify the one used for the  $p = 1$  case in the persistent landscapes section.

### 3.2 Persistence diagrams

Persistence diagrams are arguably the most common way of representing persistent homology. Let  $\mathbb{R}^{2+} = \{(a, b) \in \mathbb{R}^2 : a < b\}$ . This is the part of the plane above the diagonal. Let  $\Delta$  denote an abstract element representing the diagonal  $\{(x, x) : x \in \mathbb{R}\}$ . Let  $\mathcal{L}_{-\infty} := \{(-\infty, b) : b \in \mathbb{R}\}$  and  $\mathcal{L}_{\infty} := \{(a, \infty) : a \in \mathbb{R}\}$ . A persistence diagram is a multiset of points in  $\mathcal{L}_{\infty} \cup \mathcal{L}_{-\infty} \cup \mathbb{R}^{2+} \cup \Delta$ . For tractability we will impose some finiteness conditions, namely that only finitely many classes have infinite lifetimes and that the sum of all the finite lifetimes is finite. This restriction is not onerous in applications where generally we have finite sized data as input.

**Definition 3.1.** A persistence diagram  $X$  is a multiset of  $\mathcal{L}_{\infty} \cup \mathcal{L}_{-\infty} \cup \mathbb{R}^{2+} \cup \Delta$  such that

- The number of elements in  $X|_{\mathcal{L}_{\infty}}$  and  $X|_{\mathcal{L}_{-\infty}}$  are finite



$$\bullet \sum_{(x_i, y_i) \in X|_{\mathbb{R}^2_+}} (y_i - x_i) < \infty$$

- There are countably infinite copies of an abstract element representing the diagonal in the plane which we denote by  $\Delta$

Let  $\mathcal{D}$  denote the space of all persistence diagrams. We will consider a family of metrics which are analogous to the  $p$ -Wasserstein distances on the space of probability measures and to the  $L^p$  distances on the space of functions on a discrete set.  $\mathbb{R}^{2+}$  inherits natural  $L^p$  distances from  $\mathbb{R}^2$ . For  $p \in [1, \infty)$  we have

$$\|(a_1, b_1) - (a_2, b_2)\|_p^p = |a_1 - a_2|^p + |b_1 - b_2|^p \text{ and } \|(a_1, b_1) - (a_2, b_2)\|_\infty = \max\{|a_1 - a_2|, |b_1 - b_2|\}.$$

Recall that  $\Delta$  represents the diagonal in  $\mathbb{R}^2$ . With a slight abuse of notation we write  $\|(a, b) - \Delta\|_p$  to denote the shortest  $L^p$  distance from  $(a, b)$  in to a point in the diagonal set in  $\mathbb{R}^2$ . Thus

$$\|(a, b) - \Delta\|_p = \inf_{t \in \mathbb{R}} \|(a, b) - (t, t)\|_p = 2^{\frac{1}{p}-1} |b - a|$$

for  $p < \infty$ , and  $\|(a, b) - \Delta\|_\infty = \inf_{t \in \mathbb{R}} \|(a, b) - (t, t)\|_\infty = |y - x|/2$ . Both  $\mathcal{L}_{-\infty}$  and  $\mathcal{L}_\infty$  inherit natural  $L^p$  distances from the  $L^p$  metric on  $\mathbb{R}$ ;  $\|(-\infty, b_1) - (-\infty, b_2)\|_p = |b_1 - b_2|$  and  $\|(a_1, \infty) - (a_2, \infty)\|_p = |a_1 - a_2|$ . We should also think of  $\mathcal{L}_{-\infty}$ ,  $\mathcal{L}_\infty$  and  $\mathbb{R}^{2+} \cup \Delta$  as three separate disjoint parts of a larger space.

Given persistence diagrams  $X$  and  $Y$  we can consider all the bijections from the set of off-diagonal points and copies of  $\Delta$  in  $X$ , to the set of off-diagonal points and copies of  $\Delta$  in  $Y$ . This set is non-empty as it contains the bijection which matches everything to a copy of  $\Delta$  in the other diagram. Each bijection provides a transport plan from  $X$  to  $Y$ . Analogous to the definition of Wasserstein distances, we will define our family of metrics in terms of the cost of most efficient transport plan.

For each  $p \in [1, \infty)$  define

$$d_p(X, Y) = \left( \inf_{\text{bijections } \phi: X \rightarrow Y} \sum_{x \in X} \|x - \phi(x)\|_p^p \right)^{1/p}.$$

and  $d_\infty(X, Y) = \inf_{\text{bijections } \phi: X \rightarrow Y} \sup_{x \in X} \|x - \phi(x)\|_\infty$ .

These distances may be infinite - for example if  $X$  and  $Y$  contain a different number of points in  $\mathcal{L}_\infty$  then  $d_p(X, Y) = \infty$  for all  $p$ .

In theory, for every pair  $p, q \in [1, \infty]$  one could construct a distance function of the form

$$\inf_{\phi: X \rightarrow Y} \left( \sum_{x \in X} \|x - \phi(x)\|_q^p \right)^{1/p}$$

with  $p$  and  $q$  different. Some of the computational topology literature uses a family of metrics  $d_{W_p}$  where  $p$  varies but  $q = \infty$  is fixed. The families  $\{d_p\}$  and  $\{d_{W_p}\}$  share many properties. The metrics  $d_p$  and  $d_{W_p}$  are bi-Lipschitz equivalent as for any  $x, y \in \mathbb{R}^2$  we have  $\|x - y\|_\infty \leq \|x - y\|_p \leq 2\|x - y\|_\infty$ , implying  $d_{W_p}(X, Y) \leq d_p(X, Y) \leq 2d_{W_p}(X, Y)$ . Any stability results for  $\{d_p\}$  or  $\{d_{W_p}\}$  would extend (with minor changes in constant) to stability results for the other.

We feel that the choice of setting  $q = p$  is cleaner in theory and in practice. The coordinates of the points within a persistence diagram have particular meanings; one is the birth time and one is the death time. They are often infinitesimally independent (even though not globally so). For example, if we have generated our persistence diagram from the distance function to a point cloud then each persistence class has its birth and death time (infinitesimally) determined by the location of two pairs of points which are often distinct. Whenever these pairs are distinct, moving any of these four points will change either the birth or the death but not both. The distinctness of the treatment of birth and death times as separate qualities may seem more philosophically pleasing to the reader in the setting of barcodes.

Unfortunately the geometry of the space of persistence diagrams is complicated and statistical methods not easy to apply. For example, there are challenges even in computing the mean or median of a finite samples (see [?, ?]). Given this it is perhaps not surprising that the space of persistence diagrams is not of negative type (let alone of

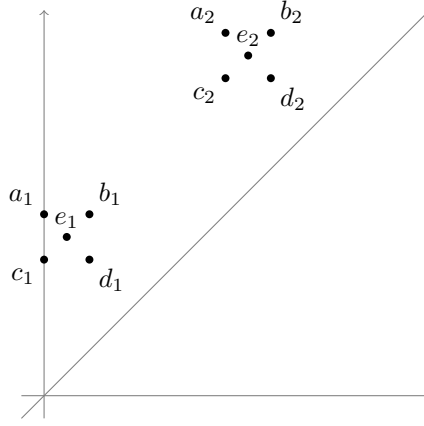


Figure 2: The off-diagonal points used in the persistence diagrams in the counterexamples for  $p \leq 2.4$ .

diagram	off-diagonal points	weight	diagram	off-diagonal points	weight
$x_1$	$\{a_1, b_1, a_2, d_2\}$	1	$y_1$	$\{a_1, d_1, a_2, b_2\}$	-1
$x_2$	$\{a_1, c_1, a_2, d_2\}$	1	$y_2$	$\{a_1, d_1, a_2, c_2\}$	-1
$x_3$	$\{b_1, d_1, a_2, d_2\}$	1	$y_3$	$\{a_1, d_1, b_2, d_2\}$	-1
$x_4$	$\{c_1, d_1, a_2, d_2\}$	1	$y_4$	$\{a_1, d_1, c_2, d_2\}$	-1
$x_5$	$\{a_1, b_1, b_2, c_2\}$	1	$y_5$	$\{b_1, c_1, a_2, b_2\}$	-1
$x_6$	$\{a_1, c_1, b_2, c_2\}$	1	$y_6$	$\{b_1, c_1, a_2, c_2\}$	-1
$x_7$	$\{b_1, d_1, b_2, c_2\}$	1	$y_7$	$\{b_1, c_1, b_2, d_2\}$	-1
$x_8$	$\{c_1, d_1, b_2, c_2\}$	1	$y_8$	$\{b_1, c_1, c_2, d_2\}$	-1

Table 1: Counterexample for  $p < 2.4$ . The off-diagonal points are those shown in Figure 2

strong negative type) under the bottleneck or any of the Wasserstein metrics. Although this has been indirectly mentioned or suggested before (notably in [18] and [7]), we include here explicit counterexamples for completeness.

**Theorem 3.2.** *The space of persistence diagrams is not of negative type under the bottleneck or any of the Wasserstein metrics.*

*Proof.* We will need to construct two different counterexamples for the different  $p$ -Wasserstein metrics; one for small  $p$  and one for large  $p$ . Note that the bottleneck metric is the case where  $p = \infty$ .

For small  $p$ , consider two separate squares with unit edge length that are sufficiently far apart as displayed in Figure 2. Each persistence diagram will be a union of a pair of corners sharing an edge in one of the squares and then a pair of corners diagonally opposite each other on the other square. We can then weight the diagrams by which square contains diagonally opposite points. A list of the diagrams is in Table 1.

We have the following distance matrix for within group distances (that is the matrix  $(d_p(x_i, x_j))_{i,j}$  which is the same as the matrix  $(d_p(y_i, y_j))_{i,j}$  by symmetry):

$$\begin{bmatrix}
 0 & 2^{1/p} & 2^{1/p} & 2^{1/p} & 2^{1/p} & 4^{1/p} & 4^{1/p} & 4^{1/p} \\
 2^{1/p} & 0 & 2^{1/p} & 2^{1/p} & 4^{1/p} & 2^{1/p} & 4^{1/p} & 4^{1/p} \\
 2^{1/p} & 2^{1/p} & 0 & 2^{1/p} & 4^{1/p} & 4^{1/p} & 2^{1/p} & 4^{1/p} \\
 2^{1/p} & 2^{1/p} & 2^{1/p} & 0 & 4^{1/p} & 4^{1/p} & 4^{1/p} & 2^{1/p} \\
 2^{1/p} & 4^{1/p} & 4^{1/p} & 4^{1/p} & 0 & 2^{1/p} & 2^{1/p} & 2^{1/p} \\
 4^{1/p} & 2^{1/p} & 4^{1/p} & 4^{1/p} & 2^{1/p} & 0 & 2^{1/p} & 2^{1/p} \\
 4^{1/p} & 4^{1/p} & 2^{1/p} & 4^{1/p} & 2^{1/p} & 2^{1/p} & 0 & 2^{1/p} \\
 4^{1/p} & 4^{1/p} & 4^{1/p} & 2^{1/p} & 2^{1/p} & 2^{1/p} & 2^{1/p} & 0
 \end{bmatrix}$$

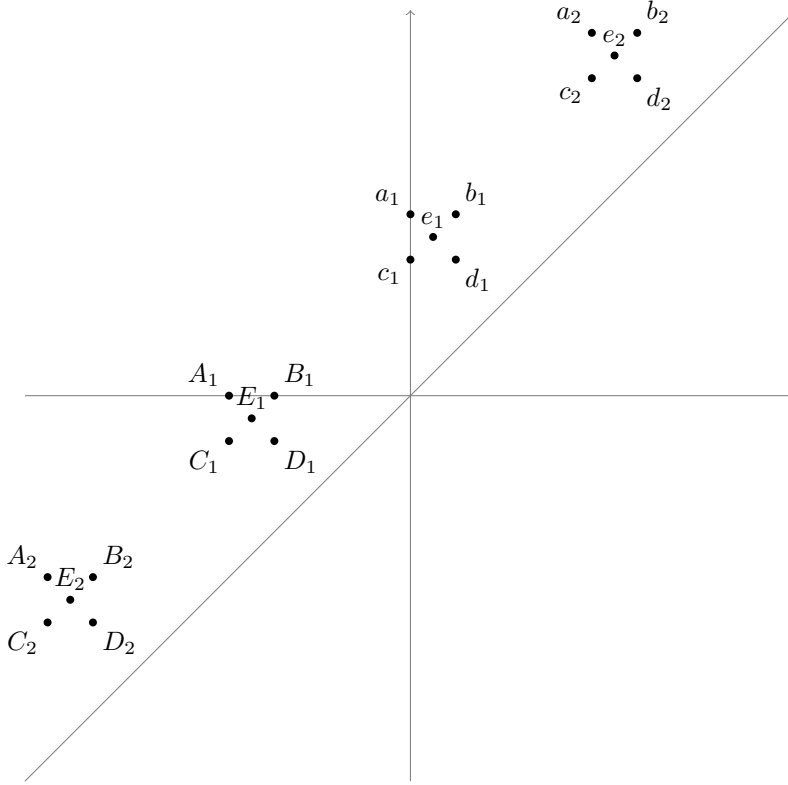


Figure 3: The off-diagonal points used in the persistence diagrams in the counterexamples for  $p \geq 2.4$ .

308 This implies that the  $\sum_{i,j} d_p(x_i, x_j) = 32 \cdot 2^{1/p} + 24 \cdot 4^{1/p}$ . Similarly  $\sum_{i,j} d_p(y_i, y_j) = 32 \cdot 2^{1/p} + 24 \cdot 4^{1/p}$ .

309 Furthermore,  $d(x_i, y_j) = 2^{1/p}$  for all  $i, j$  and hence  $\sum_{i,j} d_p(x_i, y_j) = \sum_{i,j} d_p(y_i, x_j) = 64 \cdot 2^{1/p}$ .

The sum of interest, using the weighting in Table 1, is:

$$\begin{aligned} \sum_{i,j} d_p(x_i, x_j) + \sum_{i,j} d_p(y_i, y_j) - \sum_{i,j} d_p(x_i, y_j) - \sum_{i,j} d_p(y_i, x_j) \\ = 64 \cdot 2^{1/p} + 48 \cdot 4^{1/p} - 128 \cdot 2^{1/p} \\ = 48 \cdot 4^{1/p} - 64 \cdot 2^{1/p}. \end{aligned}$$

310 Now  $48 \cdot 4^{1/p} - 64 \cdot 2^{1/p} > 0$  exactly when  $p < \ln(2)/\ln(4/3)$  which holds when  $p < 2.409$ . Thus this is a  
311 counterexample showing that persistence diagrams with  $W_p$ ,  $p < 2.409$ , is not of negative type.

312 We now will construct a counterexample for space of persistence diagrams under  $p$ -Wasserstein distance with  
313  $p \geq 2.4$ . For large  $p$ , consider separate squares with unit edge length that are sufficiently far apart as displayed in  
314 Figure 3.

315 We will construct our counterexample with persistence diagrams containing points listed in Figure 3. We will have  
316 two sets of persistence diagrams  $X$  and  $Y$  and we will be giving a weight of 1 to all the persistence diagrams in  $X$   
317 and a weight of  $-1$  to all the persistence diagrams in  $Y$ .

318 Each persistence diagram in  $X$  will have 4 off-diagonal points; one corner point from each of the squares labelled  
319 with upper case letters, and  $e_1$  and  $e_2$ . An example is  $\{A_1, B_2, e_1, e_2\}$ . There are a total of 16 such persistence  
320 diagrams.

321 Each persistence diagram in  $Y$  will have 4 off-diagonal points; one corner point from each of the squares labelled  
322 with lower case letters, and  $E_1$  and  $E_2$ . An example is  $\{c_1, c_2, E_1, E_2\}$ .

same corner	share an edge	diagonally opposite corners	example diagram	number of such $x \in X$	$d_p(x, x')$
2	0	0	$\{A_1, A_2, e_1, e_2\}$	1	0
1	1	0	$\{A_1, B_2, e_1, e_2\}$	4	1
1	0	1	$\{A_1, D_2, e_1, e_2\}$	2	$2^{1/p}$
0	2	0	$\{B_1, C_2, e_1, e_2\}$	4	$2^{1/p}$
0	1	1	$\{B_1, D_2, e_1, e_2\}$	4	$3^{1/p}$
0	0	2	$\{D_1, D_2, e_1, e_2\}$	1	$4^{1/p}$

Table 2: Table of distances  $d_p(x, x')$  for  $x \in X$  and  $x' = \{A_1, A_2, e_1, e_2\}$ . The off-diagonal points are those shown in Figure 2.

For every pair of persistence diagrams  $(x, y)$  with  $x \in X$  and  $y \in Y$  we have  $d_p(x, y) = 8^{1/p}(0.5)$ . This implies that the total between group pairwise distances are  $32 \cdot 16 \cdot 8^{1/p}(0.5)$ .

To compute the within group distances we first observe that the symmetry of the counterexample ensures that the sum of distance  $\sum_{x \in X} d_p(x, x')$  is the same for all  $x' \in X$  and that this is also the same as  $\sum_{y \in Y} d_p(y, y')$  for all  $y' \in Y$ . This means we can compute for a fixed  $x' \in X$ . We can split the remaining  $x \in X$  into cases depending on how many of the off-diagonal points in the persistence diagrams are the same as that in  $x'$ , are on the same edge of the corresponding square as that in  $x'$ , or are diagonally opposite corners of the corresponding square. We describe this distribution in Table 2, giving example persistence diagrams.

Using this table we can calculate  $\sum_{x \in X} d_p(x, x') = 4 + 6 \cdot 2^{1/p} + 4 \cdot 3^{1/p} + 4^{1/p}$ . To prove this is a counterexample we need to show that

$$32 \cdot (4 + 6 \cdot 2^{1/p} + 4 \cdot 3^{1/p} + 4^{1/p}) - 32 \cdot 16 \cdot 8^{1/p}(0.5) > 0.$$

This is equivalent to  $4 + 6 \cdot 2^{1/p} + 4 \cdot 3^{1/p} + 4^{1/p} > 8$  and by dividing through by  $8^{1/p}$  this is equivalent to the condition that

$$4(1/8)^{1/p} + 6(1/4)^{1/p} + 4(3/8)^{1/p} + (1/2)^{1/p} > 8. \quad (3.1)$$

Now  $\lambda^{1/p}$  is an increasing function in  $p$ , when  $\lambda < 1$  and  $p > 1$ . Thus for all  $p \geq 2.4$  we know  $(1/8)^{1/p} \geq (1/8)^{1/2.4} > 0.42$ ,  $(1/4)^{1/p} \geq (1/4)^{1/2.4} > 0.56$ ,  $(3/8)^{1/p} \geq (3/8)^{1/2.4} > 0.66$  and  $(1/2)^{1/p} \geq (1/2)^{1/2.4} > 0.74$ . Together these imply that

$$4(1/8)^{1/p} + 6(1/4)^{1/p} + 4(3/8)^{1/p} + (1/2)^{1/p} > 4 \cdot 0.42 + 6 \cdot 0.56 + 4 \cdot 0.66 + 0.74 = 8.42$$

and (3.1) holds for all  $p \geq 2.4$ . □

### 3.3 Persistence Landscapes

Recall that  $H_*(a, b) := Z_*(K_a)/(B_*(K_b) \cap Z_*(K_a))$  is the space of homology classes that exist in  $H_*(K_a)$  are still distinct when thought of as elements of  $H_*(K_b)$ . For  $a \leq b$  let  $\beta^{a,b} = \dim(H_*(a, b))$ . We can think of  $\beta_*$  as a persistent version of the classical Betti numbers. Indeed when  $a = b$  then it is the Betti number of  $K_a$ . Notably persistent Betti numbers are non-negative integer valued functions. Furthermore, when  $a \leq b \leq c \leq d$  then  $\beta^{a,d} \leq \beta^{c,d}$ . We can construct the persistence landscape as a sequence of functions which together completely describe the “level sets” of these integer values.

**Definition 3.3.** The *persistence landscape* is a function  $\lambda : \mathbb{N} \times \mathbb{R} \rightarrow \overline{\mathbb{R}}$  where  $\overline{\mathbb{R}}$  denotes the extended real numbers,  $[\infty, \infty]$ . Alternatively, it may be thought of as a sequence of functions  $\lambda_k : \mathbb{R} \rightarrow \overline{\mathbb{R}}$ , where,  $\lambda_k(t) = \lambda(k, t)$ . Define

$$\lambda_k(t) = \sup\{m \geq 0 \mid \beta^{t-m, t+m} \geq k\}.$$

The persistence landscapes constructed from persistence homology lie in a function space. We can consider the  $L^p$  space of these functions with  $L^p$ -norm

$$\|\lambda\|_p^p = \sum_{k=1}^{\infty} \|\lambda_k\|_p^p$$

341 where  $\lambda_k(t) = \lambda(k, t)$  and  $1 \leq p \leq \infty$ .

342 **Theorem 3.4.** *We can prove the following statements about which metrics for the space of persistence landscapes*  
 343 *is of negative type and of strong negative type.*

- 344 (a) *The space of persistence landscapes with the  $L^2$  norm of strong negative type.*
- 345 (b) *The space of persistence landscapes with the  $L^p$  norm of negative type when  $1 \leq p \leq 2$*
- 346 (c) *The space of persistence landscapes with the  $L^1$  norm is not of strong negative type, even when restricting to*  
 347 *persistence landscapes that arise from persistence diagrams.*
- 348 (d) *The space of persistence landscapes with the  $L^\infty$  norm is not of negative type, even when restricting to*  
 349 *persistence landscapes that arise from persistence diagrams.*

350 *Proof.* (a) The space of persistence landscapes with the  $L^2$  norm form a separable Hilbert space. Applying  
 351 Theorem 2.9 shows it is of strong negative type.

352 (b) As discussed in [5] these function spaces are  $L^p$  function spaces. From Theorem 3.6 in [16] we know that  
 353 these are of negative type when  $1 \leq p \leq 2$ .

(c) The space of persistence landscapes with  $p = 1$  norm is of negative type but not of strong negative type. We  
 can construct a counterexample using only distributions of landscapes that arise from persistent homology.  
 To this end it is sufficient to provide appropriate barcodes, each with finitely many bars, as every such  
 barcode can be realised. Let

$$\begin{aligned} X_1 &= I_{[0,1)} \oplus I_{[3,4)}, & Y_1 &= I_{[0,1)} \oplus I_{[1,2)}, \\ X_2 &= I_{[1,2)} \oplus I_{[2,3)}, & Y_2 &= I_{[2,3)} \oplus I_{[3,4)}, \end{aligned}$$

354 Since all the bars in each barcode are disjoint only the first persistence landscape is non-zero. We have  
 355  $d(X_1, X_2) = 2 = d(Y_1, Y_2)$  and  $d(X_i, Y_j) = 1$  for all  $i, j$ . If we weight each of the  $X_i$  with 1 and the  $Y_i$  by  $-1$   
 356 then  $\sum \alpha_k \alpha_l d(Z_k, Z_l) = 0$  which means that the space of persistence landscapes with  $p = 1$  norm is of  
 357 non-strict negative type.

(d) For  $p = \infty$  the space of persistence landscapes is not of negative type. We can construct a counterexample  
 using only distributions of landscapes that arise from persistent homology. Again we can to this via  
 examples of barcodes. Let

$$\begin{aligned} X_1 &= I_{[0,2)} \oplus I_{[6.5,7.5)} \oplus I_{[8.5,9.5)} \oplus I_{[10.5,11.5)}, & Y_1 &= I_{[0.5,1.5)} \oplus I_{[2.5,3.5)} \oplus I_{[4.5,5.5)} \oplus I_{[6,8)}, \\ X_2 &= I_{[2,4)} \oplus I_{[6.5,7.5)} \oplus I_{[8.5,9.5)} \oplus I_{[10.5,11.5)}, & Y_2 &= I_{[0.5,1.5)} \oplus I_{[2.5,3.5)} \oplus I_{[4.5,5.5)} \oplus I_{[8,10)}, \\ X_3 &= I_{[4,6)} \oplus I_{[6.5,7.5)} \oplus I_{[8.5,9.5)} \oplus I_{[10.5,11.5)}, & Y_3 &= I_{[0.5,1.5)} \oplus I_{[2.5,3.5)} \oplus I_{[4.5,5.5)} \oplus I_{[10,12)}. \end{aligned}$$

358 Since all the bars in each barcode are disjoint only the first persistence landscape is non-zero.

359 It is straightforward to compute the  $L^\infty$  distances between the corresponding persistence landscapes. Let  
 360  $pl(Z)$  denote the persistence landscape of  $Z$ . We see that  $d_\infty(pl(X_i), pl(X_j)) = 1 = d_\infty(pl(Y_i), pl(Y_j))$  when  
 361  $i \neq j$  and  $d_\infty(pl(X_i), pl(Y_j)) = 0.5$  for all  $i, j$ . If we weight each of the  $X_i$  with 1 and the  $Y_i$  by  $-1$  we get  
 362 our counterexample showing that the space of persistence landscapes with the  $L^\infty$  distance is not of negative  
 363 type.

364 □

### 365 3.4 Persistence scale space kernel

366 The persistence scale space kernel is a modification of scale space theory to a persistence diagram setting. Extra  
 367 care is needed to consider the role of the diagonal. The idea is to consider the heat kernel with an initial heat

energy of Dirac masses at each of the points in the persistence diagram with the boundary condition that it is zero on the diagonal. There is a parameter of the time the diffusion takes place. More formally, it is defined in [18] as follows.

**Definition 3.5.** Let  $\mathbb{R}^{2+} = \{x = (x_1, x_2) \in \mathbb{R}^2 : x_1 > x_2\}$  denote the space above the diagonal, and let  $\delta_p$  denote a Dirac delta centered at the point  $p$ . For a given persistence diagram  $D$ , we now consider the solution  $u : \mathbb{R}^{2+} \times \mathbb{R}_{\geq 0} \rightarrow \mathbb{R}$ ,  $(x, t) \mapsto u(x, t)$  of the partial differential equation

$$\begin{aligned} \Delta_x u &= \partial_t u && \text{in } \mathbb{R}^{2+} \times \mathbb{R}_{>0}, \\ u &= 0 && \text{on } \partial\mathbb{R}^{2+} \times \mathbb{R}_{\geq 0}, \\ u &= \sum_{p \in D} \delta_p && \text{on } \mathbb{R}^{2+} \times \{0\}. \end{aligned}$$

The persistence scale space kernel at scale  $\sigma > 0$  is then defined to be  $k_\sigma(D) := u|_{t=\sigma}$ .

These  $k_\sigma(D)$  lie in  $L_2(\mathbb{R}^{2+})$  whenever  $D$  has finitely many points.

It has a nice closed expression using a clever observation that it is the restriction of the solution of a PDE with an initial condition where below the diagonal we start with the negative of the Dirac masses over the reflection of the points in the diagram above the diagonal. For  $x \in \mathbb{R}^{2+}$  and  $t > 0$  we have

$$k_t(D)(x) = u(x, t) = \frac{1}{4\pi t} \sum_{(a,b) \in D} \exp\left(\frac{-\|x - (a, b)\|^2}{4t}\right) - \exp\left(\frac{-\|x - (b, a)\|^2}{4t}\right).$$

The metric for the space of persistence scale shape kernels is that of  $L^2(\mathbb{R}^{2+})$ . The closed form for the persistence scale space kernel allows a closed form of the pairwise distances in terms of the points in the original diagrams. In particular for diagrams  $F$  and  $G$  and fixed  $\sigma > 0$ , this distance can be written in terms of a kernel  $k_\sigma(F, G)$ . where

$$k_\sigma(F, G) = \frac{1}{8\pi\sigma} \sum_{(a,b) \in F} \sum_{(c,d) \in G} \exp\left(\frac{-\|(a, b) - (c, d)\|^2}{8\sigma}\right) - \exp\left(\frac{\|(a, b) - (d, c)\|^2}{8\sigma}\right)$$

and the corresponding distance function is  $d(k_\sigma(F), k_\sigma(G)) = (k_\sigma(F, F) + k_\sigma(G, G) - 2k_\sigma(F, G))^{\frac{1}{2}}$ .

Observe that  $L^2(\mathbb{R}^{2+})$  is a separable Hilbert space. This implies we can apply Theorem 2.9 to say it is of strong negative type.

**Corollary 3.6.** *The space of persistence scale shape kernels is of strong negative type.*

### 3.5 Sliced Wasserstein kernel distance

The Sliced Wasserstein distance between persistence diagrams, introduced in [7], is a modification of the sliced Wasserstein distance between measures. This modification is analogous to that used to define Wasserstein distances between persistence diagrams. A “slice” here is a straight line through the origin. The distance between persistence diagrams  $X$  and  $Y$  with respect to this slice is the 1-Wasserstein distance of the projection of the points in each persistence diagram onto this line (adding appropriate points on the diagonal). We then integrate over all the lines through the origin to get the total distance. More formally the definition in [7] is as follows.

**Definition 3.7.** Given  $\theta \in \mathbb{R}^2$  with  $\|\theta\|_2 = 1$ , Let  $L(\theta)$  denote the line  $\{\lambda\theta : \lambda \in \mathbb{R}\}$ , and let  $\pi_\theta : \mathbb{R}^2 \rightarrow L(\theta)$  be the orthogonal projection onto  $L(\theta)$ . Let  $Dg_1$  and  $Dg_2$  be two persistence diagrams and let  $\mu_1^\theta = \sum_{p \in Dg_1} \Delta_{\pi_\theta(p)}$  and  $\mu_2^\theta = \sum_{p \in Dg_2} \Delta_{\pi_\theta(p)}$ , and similarly for  $\mu_2^\theta$ , where  $\pi_\Delta$  is the orthogonal projection onto the diagonal. Then, the *Sliced Wasserstein distance* is defined as:

$$SW(Dg_1, Dg_2) := \frac{1}{2\pi} \int_{S^1} \mathcal{W}(\mu_1^\theta + \mu_{2\Delta}^\theta, \mu_2^\theta + \mu_{1\Delta}^\theta) d\theta$$

Here the 1-Wasserstein distance  $\mathcal{W}(\mu, \nu)$  is defined as  $\inf_{P \in \Pi(\mu, \nu)} \int \int_{\mathbb{R} \times \mathbb{R}} |x - y| P(dx, dy)$  where  $\Pi(\mu, \nu)$  is the set of measures on  $\mathbb{R}^2$  with marginals  $\mu$  and  $\nu$ .

It was shown in [7] that the Sliced Wasserstein distance is conditionally negative semidefinite on the space of finite and bounded persistence diagrams. This is equivalent to the condition of being of negative type. It is an open question as to whether the Sliced Wasserstein metric is of strong negative type.

In order to get a Hilbert space structure, the authors in [7] construct a kernel, with bandwidth parameter  $\sigma > 0$ , in the standard way (see [26]). They construct a kernel

$$k_\sigma(Dg_1, Dg_2) = -\exp\left(\frac{-SW(Dg_1, Dg_2)}{2\sigma^2}\right)$$

The distance function  $d_{kSW}$  with

$$d_{kSW}(dg_1, Dg_2)^2 = k_\sigma(Dg_1, Dg_1) + k_\sigma(Dg_2, Dg_2) - 2k_\sigma(Dg_1, Dg_2)$$

does define a Hilbert space.

If this reproducing kernel Hilbert space is separable then it will be of strong negative type. This separability property is an open question.

## 4 Distance correlation between different topological summaries

For the simulations and elevation data studied later we used the Approximate Wasserstein distances with “Hera”, see [11] to compute the Wasserstein and the bottleneck distances between the persistence diagrams. Persistence landscapes computations were done using the persistence landscapes toolkit, see [6].

The differences in metric can dramatically affect the statistical analysis of a data set. It is important to choose a summary such that the differences in the raw data that are of interest are reflected in the distances between their corresponding topological summaries.

The key idea in this section is to take the same random object and then to record different topological summaries of it. Once we compute its persistent homology we can construct its persistence diagram, or its persistence landscape, etc. Although they contain the same persistent homology information, they lie in different metric spaces. We then compare the pairwise distances using distance correlation.

The inputs we are considering in this simulation study are a variety of standard families of random filtrations of cell complexes. These include variations on random abstract complexes and random geometric complexes.

### 4.1 Erdos-Renyi

In this simulation we construct random graphs over 100 vertices where each edge had independently chosen weights. We then get a filtration of graphs where we include all edges with weight less than the filtration parameter. We then constructed the corresponding filtration of the flag complexes. This was performed 100 times to construct samples of the distribution of persistent homology for such complexes using [3]. An example persistence diagram is shown in Figure 4.1. We then computed the distance correlation between the different topological summaries which is also shown in Figure 4.1.

### 4.2 Directed Erdos-Renyi

In this simulation we construct random directed graphs over 100 vertices where each directed edge had independently chosen weights. We then get a filtration of directed graphs where we include all the directed edges

with weight less than the filtration parameter. We then constructed the corresponding filtration of directed flag complexes (see [19]). This was performed 100 times to construct samples of the distribution of persistent homology for such complexes using [14]. An example persistence diagram is shown in Figure 4.2. We then computed the distance correlation between the different topological summaries which is also shown in Figure 4.2.

### 4.3 Geometric Random Complexes for points sampled on a torus

In this simulation we uniformly randomly sampled 100 points independently from a torus lying in  $\mathbb{R}^4$ . We then built the  $\alpha$ -complex over this set of points. This was performed 100 times to construct samples of the distribution of persistent homology for such complexes. An example persistence diagram is in Figure 4.3. We then computed the sample distance correlation between the different topological summaries which is shown in Figure 4.3.

The computation of the alpha complexes and the persistent homology was done using [10].

### 4.4 Geometric Random Complexes for point sampled on a unit cube

In this simulation we uniformly randomly sampled 500 points independently from a the unit cube  $([0, 1]^3)$ . We then built the  $\alpha$  complex over this set of points. This was performed 100 times to construct samples of the distribution of persistent homology for such complexes. An example persistence diagram is in Figure 4.4. We then computed the distance correlation between the different topological summaries which is shown in Figure 4.4.

The computation of the alpha complexes and the persistent homology was done using [10].

## 5 Distance correlation to another parameter

Another avenue is to consider models with a parameter. We may hope that the topological summary captures this parameter in a statistically measurable way. Alternatively we may be interested in whether the summary is independent of this parameter. We can use distance correlation to quantify how well the distances between some topological summaries relate to the differences in that parameter. The varying performances of the different topological summaries in correlating to the parameter highlights how the the choice of topological summary has statistical significance.

In this study we consider a model of random filtrations with a parameter  $\gamma \in [0, 1]$  such that for  $\gamma = 0$  we have a geometric Rips filtration, and for  $\gamma = 1$  we have an Erdos-Renyi Rips filtration. We compute the distance correlation of the topological summaries to this parameter  $\gamma$ . We also consider some topographic data from maps of Norway and compute the distance correlation of topological summaries of the elevation function to geographic measurements of geodesic measurements between the locations of the maps and also the distance correlation to the Terrain Roughness Index.

### 5.1 Fully Erdos-Renyi to fully Geometric Random

We considered a random model for filtrations of simplicial complexes is a parameterised mixture of the Geometric and the ER models. The parameter  $\gamma \in [0, 1]$  is such that when  $\gamma = 1$  we generated ER and when  $\gamma = 0$  we generated Random geometric.

For this simulation we first fix a parameter  $\gamma \in [0, 1]$ . Then we sampled 100 points  $V = \{x_1, \dots, x_{100}\}$  i.i.d. with uniform probability over the the unit cube. For each  $i, j$  set  $X_{ij} = \|x_i - x_j\|_2$ . We also pick  $Y_{i,j}$  independently at random from the interval  $[0, 1]$ . We then create weightings over the complete graph over  $V$  by, independently for each pair  $i, j$ , setting the weight to be  $X_{i,j}$  with probability  $\gamma$  and  $Y_{i,j}$  otherwise.



topological summary	dCov( $\cdot, \gamma$ )
persistence scale space kernel, $\sigma = 0.001$	0.96
1-Wasserstein	0.95
$L^1$ of $\beta_1$	0.95
$L^2$ of $\beta_1$	0.95
2-Wasserstein	0.94
persistence landscape $L^\infty$	0.94
persistence scale space kernel, $\sigma = 0.01$	0.93
persistence landscape $L^2$	0.92
persistence landscape $L^1$	0.92
Sliced Wasserstein kernel, $\sigma = 1$	0.66
persistence scale space kernel, $\sigma = 1$	0.60
Sliced Wasserstein kernel, $\sigma = 0.01$	0.40

Table 3: (Square roots of) distance correlation between topological summaries and the parameter  $\gamma$ .

From this random filtration of the complete graph over  $S$  we constructed the corresponding clique filtration and computed its persistent homology.

This model ranges from “fully ER” ( $\gamma = 0$ ) to “fully Rips geometric” ( $\gamma = 1$ ). We simulated this model varying  $\gamma$  from 0 to 1 (inclusive) in 100 steps and computed the distance correlation between the topological summaries and the value of interpolation parameter. These distance correlations are displayed in Table 3. The higher the distance correlation the better the topological summary reflects the effect of the parameter  $\gamma$ . We see that generally the function distances between Betti curves, Wasserstein distances and bottleneck distances between and the function distances between persistence landscapes had a higher correlation, all with a distance correlation greater than 0.9. This illustrates that these topological summaries would be good choices if we wish to do learning problems or statistical analysis with regards to this parametrised random model, such as parameter estimation. We also see the importance of the choice of bandwidth with dramatic effect on the distance correlation of the persistence scale space kernel.

## 5.2 Maps of Norway

An example using “real world” data is the analysis of digital elevation model of patches of Norway. The digital elevation model are 5 km by 5 km patches of elevation data with a longitude and latitude resolution of 10 m, and a resolution in elevation of about 1 m. The data comes from a 50 km by 50 km block of elevation data roughly centred at the city of Trondheim, Norway, courtesy of the Norwegian Mapping Authority [17]. An example patch of elevation data is displayed in Figure 5.2. We computed the persistent homology with respect to the height function via cubical complexes using [10].

We computed the distance correlation between the topological summaries and two other external measurements; the geodesic distance between the centres of the patches, and the Terrain Roughness Index. The Terrain Roughness Indicator, TRI, a very simple real-valued model (one of many) geographers and geologists use for terrain roughness. The TRI of a grid cell is the difference between the value of a cell and the mean of an 8-cell neighbourhood of surrounding cells. The grid cell TRI values are then averaged out to provide a single number for the digital elevation model. These are tabulated in Table 4. We can see that the 2-Wasserstein distance between the persistence diagrams had a higher correlation to both of these other measurements than the other topological summaries did and the bottleneck distance had the lowest distance correlation. This would indicate that 2-Wasserstein may be a more suitable topological summary for statistical analysis or learning problems for this type of topographic data if we want a summaries that reflects closeness in geographic distance and terrain ruggedness. We also see that generally the topological summaries were more closely related to the terrain ruggedness indicator than the geodesic distance between centres. This is not altogether surprising as the correlation to the geodesic centres is probably due to the latent variable of how similarly rugged the elevations nearby patches are to each other.

	dCor( $\cdot$ , TRI)	dCor( $\cdot$ , geodesic distance)
TRI	1	0.73
Geodesic dist	0.73	1
2-Wasserstein	0.93	0.74
persistence scale space kernel, $\sigma = 1$	0.74	0.64
persistence scale space kernel, $\sigma = 10$	0.75	0.63
$L^1$ of $\beta_1$	0.75	0.65
$L^2$ of $\beta_1$	0.77	0.63

Table 4: (Square roots of) distance correlation between elevation topological summaries and Terrain Ruggedness Index and the geodesic distance between samples.

## 6 Future directions

Non-parametric statistics is a fruitful area for ideas and methods for use in TDA. There are already a variety of options that only use pairwise distances including null-hypothesis testing, clustering, classification, and parameter estimation. In all these cases, we would expect that distance correlation would be a good estimator for similarity of statistical analysis.

We can perform null hypothesis testing with topological summaries via a permutation test with a loss function a function of the pairwise distances (see [22]). Intuitively, when there is a high distance correlation then the pairwise distances are correlated and the corresponding loss functions should be similar for each permutation of the labels. This implies we should expect that the  $p$ -values given a sample distribution should be close, at least with high probability. It may be possible to show that the power of the null hypothesis tests are close. An experimental and theoretical exploration of this relationship is a future direction.

We can also think of considering a modification of the permutation test for independence using distance correlation (instead of Pearson correlation). This then can be applied to topological summaries. We can get a  $p$ -value that two variables are independent by permuting one of the variables but keeping the marginal distributions the same. A high ranking of the distance correlation for the original joint distribution would indicate that the variables are not independent with high probability. Exploring the power of this method is a future direction for research.

Another non-parametric method is parameter estimation using nearest neighbours. One method for estimating a real valued parameter which is unknown on a particular sample but is known on a training set is to take a weighted average of the values of the parameter on the training set with the weighting dependent on the pairwise distances from the sample of interest to those in the training set. We would expect better estimation when the distance correlation between the samples and the parameter of interest is high. Future directions can include experimental and theoretical results here with respect to topological summaries. In particular, we would expect that we should be able to create confidence intervals for the parameter, dependent on the distance correlation. This is also an area where we should expect similar statistical analysis when the samples have high distance correlation.

Completely analogous to the above comments, clustering methods using pairwise distances should have similar results when the sets of samples have high distance correlation and future work could explore this with respect to topological summaries.

## References

- [1] Adams H, Emerson T, Kirby M, Neville R, Peterson C, Shipman P, Chepushtanova S, Hanson E, Motta F, Ziegelmeier L. “Persistence images: A stable vector representation of persistent homology.” *The Journal of Machine Learning Research*. 2017;18(1):218-252.
- [2] Anirudh R, Venkataraman V, Natesan Ramamurthy K, Turaga P. “A riemannian framework for statistical analysis of topological persistence diagrams”. In *Proceedings of the IEEE Conference on Computer Vision and Pattern Recognition Workshops*, 2016; 68-76.

- [3] Bauer U. “Ripser” software. 2016; Available from: <https://github.com/Ripser/ripser>
- [4] Biscio C, Møller J. “The accumulated persistence function, a new useful functional summary statistic for topological data analysis, with a view to brain artery trees and spatial point process applications.” 2016 *arXiv preprint* arXiv:1611.00630
- [5] Bubenik P. “Statistical Topological Data Analysis using Persistence Landscapes.” *Journal of Machine Learning Research*, 2015;16:77-102.
- [6] Bubenik P, Dlotko P. “A persistence landscapes toolbox for topological statistics.” *Journal of Symbolic Computation*. 2017 Feb 28;78:91-114.
- [7] Carrière M, Cuturi M, Oudot S., “Sliced Wasserstein Kernel for Persistence Diagrams”, *arXiv preprint*. 2017; arXiv:1706.03358v3
- [8] Carriere M, Oudot SY, Ovsjanikov M. “Stable topological signatures for points on 3d shapes.” In *Computer Graphics Forum*, 2015 Aug (Vol. 34, No. 5, pp. 1-12).
- [9] Di Fabio B, Ferri M. “Comparing persistence diagrams through complex vectors.” In *International Conference on Image Analysis and Processing*, Springer, 2015;294-305.
- [10] The GUDHI Project. *GUDHI User and Reference Manual*. The GUDHI Editorial Board; 2015
- [11] Michael Kerber, Dmitriy Morozov, and Arnur Nigmatov, “Geometry Helps to Compare Persistence Diagrams.”, ALENEX 2016.
- [12] Kusano G, Fukumizu K, Hiraoka Y. ”Kernel method for persistence diagrams via kernel embedding and weight factor.” *Journal of Machine Learning Research*. 2018; 18(189) : 1-41.
- [13] Le T, Yamada M. ”Riemannian Manifold Kernel for Persistence Diagrams.” *arXiv preprint* 2018; arXiv:1802.03569.
- [14] Lütgehetmann D. “Flagser” software. personal communication.
- [15] Lyons R. Distance covariance in metric spaces. *The Annals of Probability*. 2013;41(5):3284-305.
- [16] M. W. Meckes, Positive definite metric spaces, *Positivity* 2013; 17(3): 733-757.
- [17] Norwegian Mapping Authority. Available from: <https://www.kartverket.no/en/data/Open-and-Free-geospatial-data-from-Norway/>
- [18] Reininghaus J, Huber S, Bauer U, Kwitt R. “A Stable Multi-Scale Kernel for Topological Machine Learning”. *IEEE Conference on Computer Vision and Pattern Recognition*, 2015.
- [19] Reimann MW, Nolte M, Scolamiero M, Turner K, Perin R, Chindemi G, Dłotko P, Levi R, Hess K, Markram H. “Cliques of neurons bound into cavities provide a missing link between structure and function”. *Frontiers in computational neuroscience*. 2017 Jun 12;11:48.
- [20] Riley SJ, DeGloria, SD, Robert E, “A Terrain Ruggedness Index that quantifies topographic heterogeneity”, *Intermountain Journal of Sciences* 1999 Dec; 5 (1-4):23-27.
- [21] Robins V, Turner K. “Principal Component analysis of Persistent Homology Rank Functions with case studies of Spatial Point Patterns, Sphere Packings and Colloids.” *Physica D: Nonlinear Phenomena*, 2016 Nov 1; 334:99-117.
- [22] Robinson A, Turner K. “Hypothesis Testing for Topological Data Analysis.” *Journal of Applied and Computational Topology*, 2017 Dec 1;1(2): 241-261.
- [23] Székely GJ, Rizzo ML, Bakirov NK. “Measuring and testing dependence by correlation of distances.” *The Annals of Statistics* 2007; 35(6) 2769-2794.
- [24] Turner K, Mileyko Y, Mukherjee S, Harer J. “Fréchet means for distributions of persistence diagrams.” *Discrete & Computational Geometry*. 2014 Jul 1;52(1):44-70.

- 562 [25] Turner K. “Medians of populations of persistence diagrams.” *arXiv preprint* 2013; arXiv:1307.8300.
- 563 [26] Van Den Berg C, Christensen JP, Ressel P. *Harmonic Analysis on Semigroups: Theory of Positive Definite*  
564 *and Related Functions*. Springer Science & Business Media; 2012 Dec 6.
- 565 [27] wikipedia image. Available from:  
566 [https://en.wikipedia.org/wiki/Correlation\\_and\\_dependence#/media/File:Correlation\\_examples2.svg](https://en.wikipedia.org/wiki/Correlation_and_dependence#/media/File:Correlation_examples2.svg)
- 567 [28] wikipedia image. Available from:  
568 [https://en.wikipedia.org/wiki/Distance\\_correlation#/media/File:Distance\\_Correlation\\_Examples.svg](https://en.wikipedia.org/wiki/Distance_correlation#/media/File:Distance_Correlation_Examples.svg)
- 569 [29] Zinger AA, Kakosyan AV, Klebanov LB. “A characterization of distributions by mean values of statistics  
570 and certain probabilistic metrics”, *Journal Soviet Mathematics*. 1992; 59 (4): 914 - 920. Translated from:  
571 *Problemy Ustoichivosti Stokhasticheskikh Modelei*, Trudy Seminara, 1989, pp. 47?55.

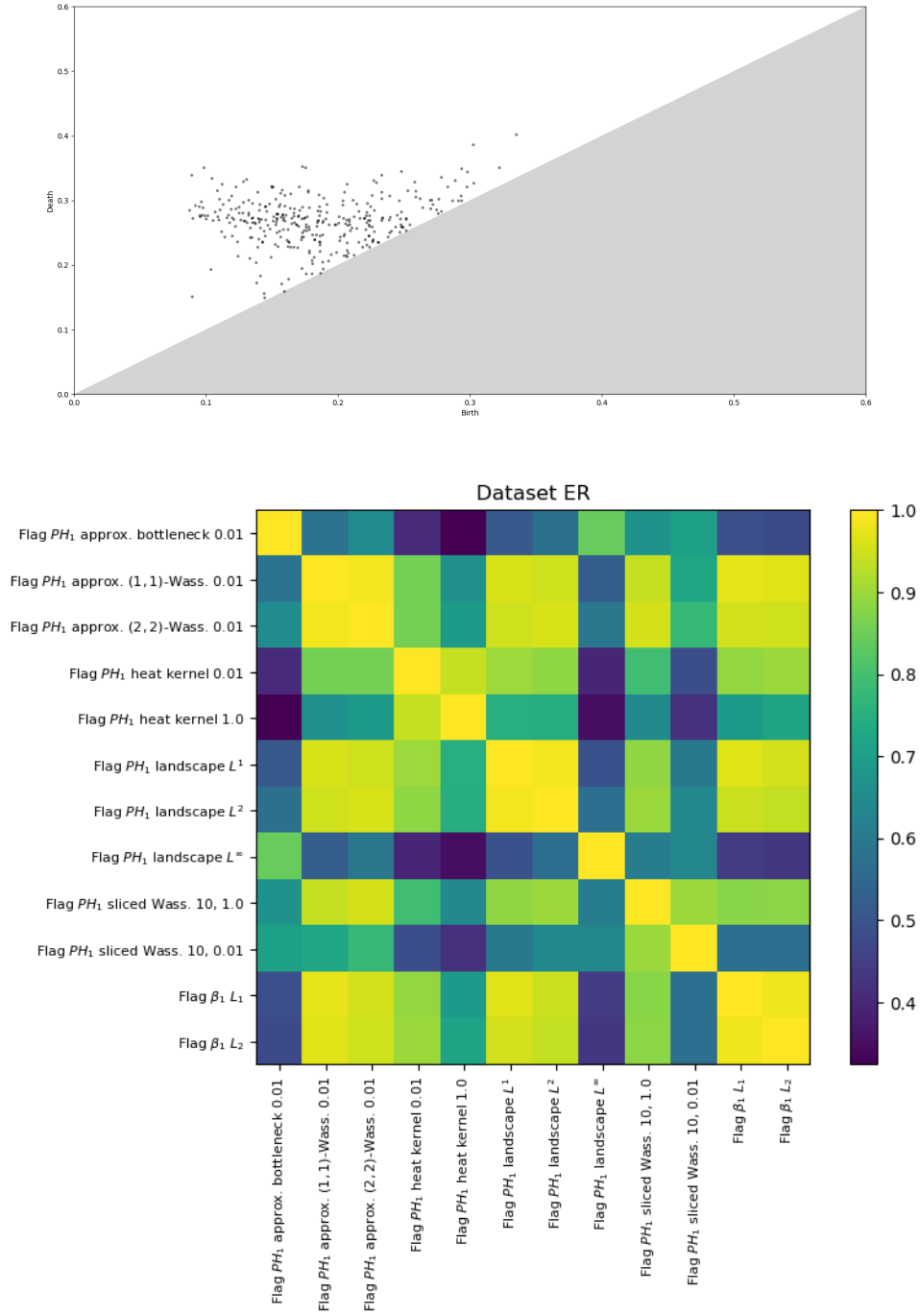


Figure 4: A typical persistence diagram and the sampled square root of distance correlation (dCor) between different topological summaries for Erdos-Renyi complexes.

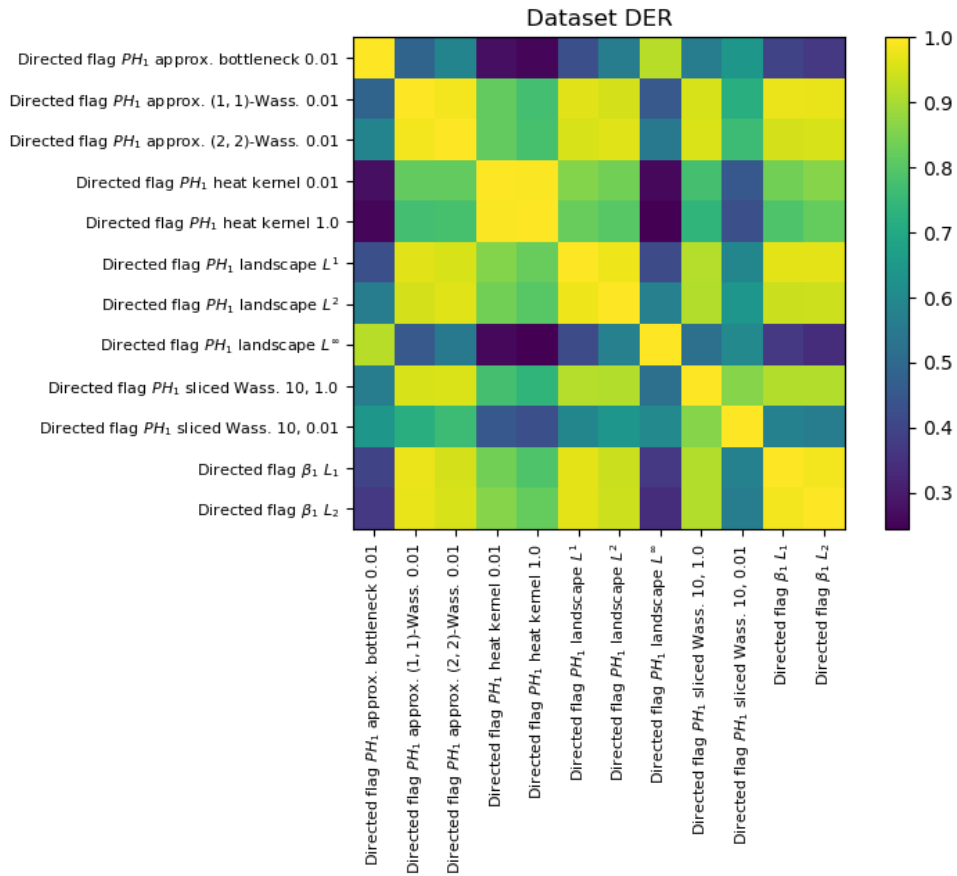
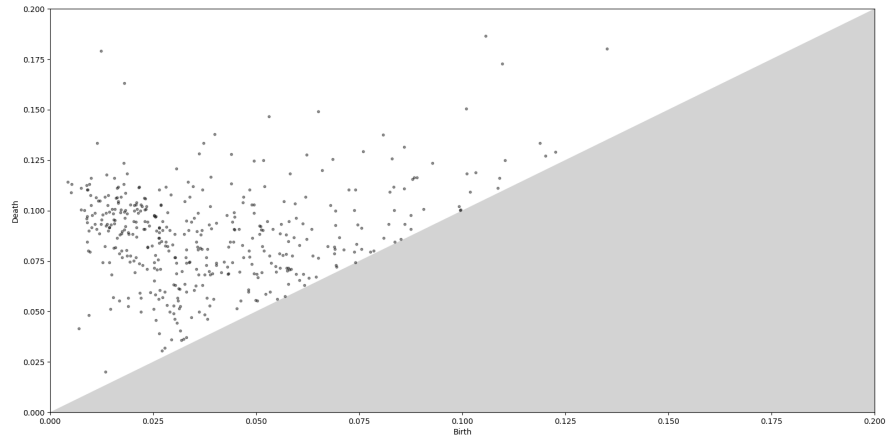


Figure 5: A typical persistence diagram and the sampled square root of distance correlation (dCor) between different topological summaries for Directed Erdos-Renyi complexes.

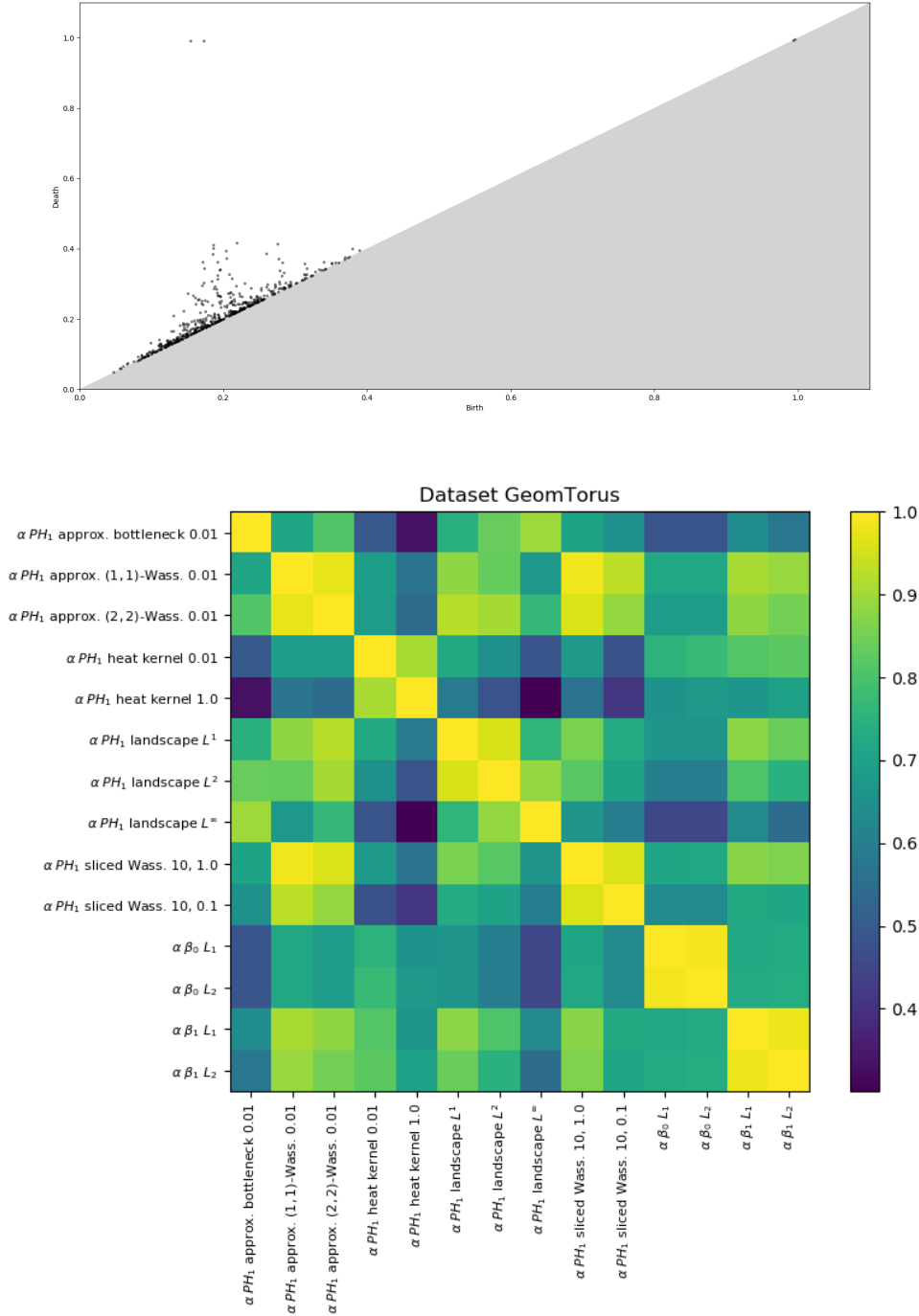


Figure 6: A typical persistence diagram and the sampled square root of distance correlation (dCor) between different topological summaries for alpha complexes built from random points clouds sampled from torus lying in  $\mathbb{R}^4$ .

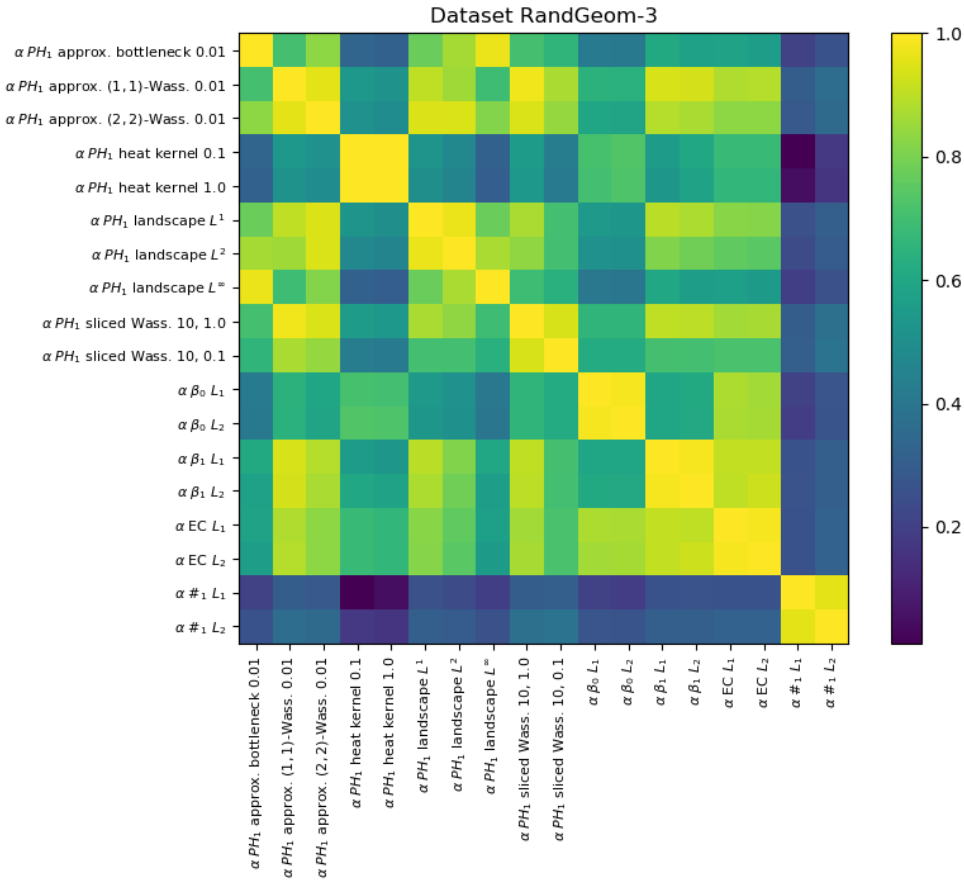
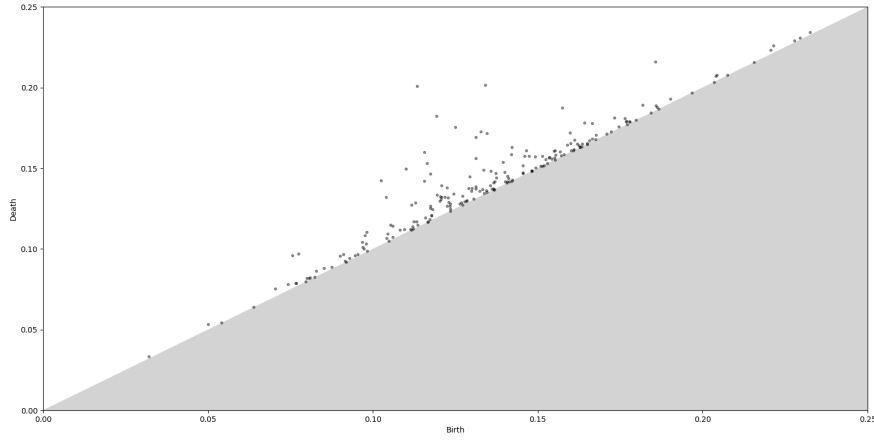


Figure 7: A typical persistence diagram and the sampled square root of distance correlation (dCor) between different topological summaries for alpha complexes built from random points clouds sampled from the unit cube.



